Catalysis Communications 11 (2010) 643–646

Contents lists available at ScienceDirect

Catalysis Communications

journal homepage: www.elsevier.com/locate/catcom

Effects of Pb dopant on structure and activity of Pd/K-OMS-2 catalysts for heterogeneous oxidative carbonylation of phenol

Xiaojun Yang [a,b], Jinyu Han [a], Zhiping Du [b], Hua Yuan [b], Fang Jin [b], Yuanxin Wu [a,b,*]

[a] School of Chemical Engineering and Technology, Tianjin University, Tianjin 300072, PR China
[b] Key Laboratory for Green Chemical Process of Ministry of Education, Wuhan Institute of Technology, Wuhan 430073, PR China

ARTICLE INFO

Article history:
Received 19 August 2009
Received in revised form 11 January 2010
Accepted 13 January 2010
Available online 18 January 2010

Keywords:
Diphenyl carbonate
Oxidative carbonylation
Cryptomelane
Hollandite-type manganese oxides
Pb dopant

ABSTRACT

Palladium catalysts supported on Pb-cation-doped manganese oxide octahedral molecular sieves were prepared and used for heterogeneous oxidative carbonylation of phenol to diphenyl carbonate in the absence of homogeneous cocatalysts. The synthesized catalysts were characterized by ICP-AES, XRD and XPS techniques. The experimental results demonstrated that an enhanced activity was obtained when Pb^{2+} entered into the tunnels of cryptomelane by replacing K^+ to form a new hollandite-type phase of $Pb_{2-x}Mn_8O_{16}$. The promotion effect of Pb dopant on activity was ascribed to the increase of low-valence Mn^{3+} and OH group, which was favor of reoxidation of Pd^0 to active Pd^{2+} species.

1. Introduction

Diphenyl carbonate (DPC) is an important starting material for producing polycarbonate. Several methods have been developed to synthesize DPC [1]. Among them, oxidative carbonylation of phenol with CO and O_2 is a simple and environmentally benign process that avoids the use of phosgene. In this catalytic reaction, two or more metallic and/or organic homogeneous cocatalysts should be added into the system in order to promote the reoxidation of reduced Pd^0 because direct oxidation of Pd^0 with gas oxygen to regenerate active Pd^{2+} species proved to be a slow process [2,3]. Although Pd complexes anchored on various supports have been developed to facilitate the recovery of homogeneous palladium catalysts [4–9], the problems in the separation and product refining still remain owing to the presence of homogeneous cocatalysts. Therefore, some researchers attempted to use metal oxides instead of homogeneous cocatalysts [2,4,5,10]. Insoluble metal oxides are easily separated and the function of reoxidation of Pd^0 is performed simultaneously.

Takagi and his coworkers discovered that PbO effectively promoted the activity in the Pd/C—$N(C_4H_9)_4Br$ system and 9.65% DPC yield was obtained in combination of CuO as a second cocatalyst [4]. But PbO was likely to react with phenol to form an organic lead compound, which meant it was a homogeneous cocatalyst in fact [10]. Although other single metal oxides, such as CuO [5], CrO_3, MoO_3, OsO_4 and RuO_3 [2], were also chosen as redox cocatalysts, the activities were not satisfactory. The best yield was only 8.9% when using 5%Pd/C as catalyst and CuO as cocatalyst. Besides, both the Pd catalyst and the Co cocatalyst were heterogenized and proven to form an effective catalytic system using layered double hydroxides as a support. Preliminary test showed a promising result as far as activity and Pd leaching is less than 5% [7]. Our research group placed emphasis on manganese oxides because only MnO_2/Mn^{2+} pair with potentials of between the potentials of Pd^{2+}/Pd^0 and $O_2 + H^+/H_2O$ pairs can oxidize Pd^0 and then be reoxidized by O_2. The Pd^0 formed was oxidized with Mn^{4+} to form Pd^{2+} and Mn^{2+}, and then Mn^{2+} was reoxidized by O_2. The dual role of manganese oxides as cocatalyst and support for the metallic parts of the catalytic system led to an easy separation process and the DPC yield achieved 10.7% [11].

As mentioned above, the activities of catalysts with metal oxides as cocatalysts are inferior to those using homogeneous cocatalysts; nevertheless the advantage of easy separation for metal oxide as cocatalysts is very attractive. Thus, an enhanced activity is essential in order to substitute for homogeneous cocatalysts, and introduction of other metal dopant into metal oxides is a powerful method. In this work, Pb was doped into potassium-containing manganese oxide octahedral molecular sieves (K-OMS-2), on which the active palladium species were loaded by a precipitation method. The supported catalysts were characterized to clarify the modification effects of Pb on structure and activity of heterogeneous catalysts.

* Corresponding author. Address: School of Chemical Engineering and Technology, Tianjin University, Tianjin 300072, PR China.
E-mail address: wyx@mail.wit.edu.cn (Y.X. Wu).

1566-7367/$ - see front matter © 2010 Elsevier B.V. All rights reserved.
doi:10.1016/j.catcom.2010.01.013

2. Experimental

2.1. Catalyst preparation

Hydrothermal, reflux, solvent free and high temperature calcination methods were used to synthesize K-OMS-2. The details of preparation were given in the literature [12]. To prepare lead-cation-doped K-OMS-2, 7000 g K-OMS-2 prepared by the reflux method was impregnated with 70.0 ml of $Pb(NO_3)_2$ aqueous solutions with different concentrations. And then the mixture was stirred for 24 h, followed by evaporation. The lead modified supports (designed as Pb-OMS-2) were obtained by calcination in a muffle furnace at 400–900 °C for 6 h.

0.042 g $PdCl_2$ was dissolved in 50.0 ml aqueous solution when the pH value was adjusted to 1.0 with concentrated hydrochloric acid. K-OMS-2 or Pb-OMS-2 was dipped into the $PdCl_2$ solution. 5.0% NaOH solution as a precipitant was dropped slowly till the pH value was kept at 9.5. After stirred for 2 h, the solid was separated by filtration, then dried at 80 °C overnight and calcined at 300 °C for 3 h. The powdery catalysts prepared were labeled as Pd/K-OMS-2 or Pd/Pb-OMS-2, respectively.

2.2. Characterization

The phase identification and crystalline structure analysis were determined by X-ray diffraction (XRD) on a PANalytical X'Pert PRO X-ray diffractometer with high-intensity Cu Kα radiation (λ = 1.54060 Å). The chemical shift and valence of element on surface were studied by X-ray photoelectron spectra (XPS) in a Perkin–Elmer PHI 1600 ESCA system with Mg Kα X-ray radiation (1253.6 eV, 250 W). The bulk chemical composition of the samples was determined by inductively coupled plasma atomic emission spectroscopy (ICP-AES) on a Perkin Elmer ELAN DRC-e instrument. Samples were dissolved in the mixture of HCl and HNO_3, and then diluted with ultrapure water.

2.3. Activity test

The oxidative carbonylation reaction was performed in a 250 ml stainless steel autoclave equipped with a magnetic stirrer. A typical reaction condition was as follows: phenol 47 g (0.5 mol), 4A molecular sieves (MS) 2 g, tetrabutylammonium bromide (TBAB) 1 g (3 mmol) and Pd (in the catalyst) 0.09 mmol were introduced into the autoclave. Then the autoclave was sealed and heated to 65 °C. Subsequently, the gas mixture of CO and O_2 (CO/O_2 = 12/1 M ratio) was charged. It must be noted that the conditions employed in this procedure fell within the explosion range of CO in O_2. After the reaction lasted for 4 h at the pressure of 4.8 MPa, the autoclave was cooled and the products were taken out. The yields of final products were determined by a capillary gas chromatography with a FID detector and a SE-54 capillary column.

3. Results and discussion

3.1. Activity studies

Table 1 shows the catalytic activities of Pd/K-OMS-2 and Pd/Pb-OMS-2 catalysts for oxidative carbonylation of phenol. As listed in Table 1, the activities of Pd/K-OMS-2 catalysts prepared by different methods were almost the same (entries 1–4). The yields of DPC varied in a narrow range of 7.5%–9.2%.

It can be also observed from Table 1 that the DPC yields of Pd/Pb-OMS-2 catalysts changed with Pb/Mn mass ratios and calcination temperatures. When the Pb/Mn mass ratio was 3/10 and the calcination temperature of Pb-OMS-2 was 700 °C, the DPC yield was up to 18.1%, indicating the best catalytic activity. The yield of Pd/Pb-OMS-2(C) was almost twice as much as that of undoped Pd/K-OMS-2 catalysts.

3.2. XRD characterization

Fig. 1 illustrates the results of XRD analysis for Pb-OMS-2 with different Pb/Mn mass ratio at the calcination temperature of 400 °C. The reference pattern of K-OMS-2 synthesized by a reflux method was given in Fig. 1a, corresponding to cryptomelane [12]. K-OMS-2 has a one-dimensional tunnel structure formed by 2 × 2 edge shared MnO_6 octahedral chains and a general composition KMn_8O_{16}. After Pb was doped into K-OMS-2 with the Pb/Mn mass ratio at 1/10, diffraction pattern of Pb-OMS-2(A1) sample (Fig. 1b) was almost identical to that of K-OMS-2. When the Pb/Mn mass ratio increased to 3/10, however, the intensity of the peak at $2\theta = 37.5^o$ was suppressed and the intensity at $2\theta = 28.7^o$ was enhanced. Fig. 1c showed that the strongest peak appeared at $2\theta = 28.7^o$, not at 37.5^o. It indicated that a new hollandite-type phase of $Pb_{2-x}Mn_8O_{16}$ generated through ion exchange in tunnels. In the light of the results of activity studies shown in Table 1 (entry 6), the reason for increasing catalytic activity might be ascribed to the formation of $Pb_{2-x}Mn_8O_{16}$ after the doping of Pb. When the Pb/Mn mass ratio was over 3/10, the crystalline phase of $Pb_3(CO_3)_2(OH)_2$, as shown in Fig. 1d, was found at $2\theta = 35.6^o$. The appearance of $Pb_3(CO_3)_2(OH)_2$ was possibly due to the reaction of CO_2 and H_2O in air with Pb^{2+}, which did not enter into tunnels. Combined with the activity of Pd catalyst supported on Pb-OMS-2(A3) (entry 7), it was found that the formation of $Pb_3(CO_3)_2(OH)_2$ was detrimental to the catalytic activity.

Table 1
Catalytic activities of palladium catalysts supported on K-OMS-2 and Pb-OMS-2.

	Support	Method of preparation	[Pb/Mn][b]	Pd[c]%	DPC Yield[d] (%)
1	K-OMS-2	Solvent free		4.92	9.2
2		Reflux		4.88	8.7
3		High temperature		4.92	8.0
4		Hydrothermal		4.79	7.5
5	Pb-OMS-2(A1)	Calcine at 400 °C, Pb/Mn[a] = 1/10	0.106	4.99	10. 0
6	Pb-OMS-2(A2)	Calcine at 400 °C, Pb/Mn = 3/10	0.321	4.87	13.2
7	Pb-OMS-2(A3)	Calcine at 400 °C, Pb/Mn = 5/10	0.546	5.00	10.3
8	Pb-OMS-2(B)	Calcine at 550 °C, Pb/Mn = 3/10	0.332	4.95	17.0
9	Pb-OMS-2(C)	Calcine at 700 °C, Pb/Mn = 3/10	0.311	4.95	18.1
10	Pb-OMS-2(D)	Calcine at 850 °C, Pb/Mn = 3/10	0.320	4.89	7.0

[a] Theoretical value of mass ratio of Pb to Mn.
[b] Mass ratio of Pb to Mn detected by ICP-AES.
[c] Actual loading of active Pd species in heterogeneous catalysts detected by ICP-AES.
[d] DPC yield based on the amount of charged phenol.

XRD was also undertaken to study the influence of calcination temperature on crystal structure for the same Pb content (shown in Fig. 2). At 550 °C, two groups of peaks were observed with the location of the most intensive peaks at 2θ of 28.7° and 32.7°, respectively, indicating that the presence of crystalline phase of a large amount of $Pb_{2-x}Mn_8O_{16}$ and a small amount of bixbyite. The peaks after 60 degrees were suppressed with the increase of temperature because $Pb_{2-x}Mn_8O_{16}$ and bixbyite generated at a high temperature. It was well known that K-OMS-2 was progressively converted into bixbyite with the increase of temperature [13]. Therefore, the growth of bixbyite crystals was observed based on the increasing intensity of the peak at $2\theta = 32.7°$ when the calcined temperature increased to 700 °C. The majority of phase remained $Pb_{2-x}Mn_8O_{16}$ and the best yield of DPC was obtained. However, at 850 °C sharp diffraction peaks were detected, suggesting a fully developed crystalline structure of bixbyite. Combined with the results of catalytic activities shown in Table 1 (entries 9 and 10), it was concluded that effective support was not bixbyite, but $Pb_{2-x}Mn_8O_{16}$.

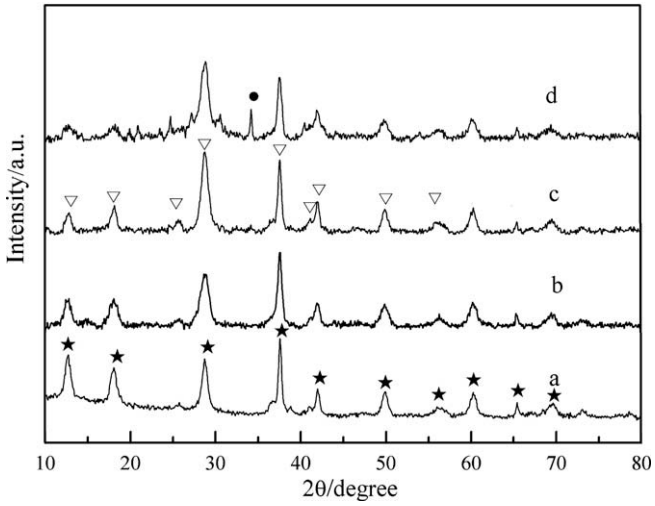

Fig. 1. XRD patterns of doped catalysts with different mass ratio of Pb to Mn. (★) KMn_8O_{16}, JCPDS file 29-1020; (▽) $Pb_{2-x}Mn_8O_{16}$, JCPDS file 42-1349; (●) $Pb_3(CO_3)_2(OH)_2$, JCPDS file 13-0131. (a) K-OMS-2 (b) Pb-OMS-2(A1), (c) Pb-OMS-2(A2) and (d) Pb-OMS-2(A3).

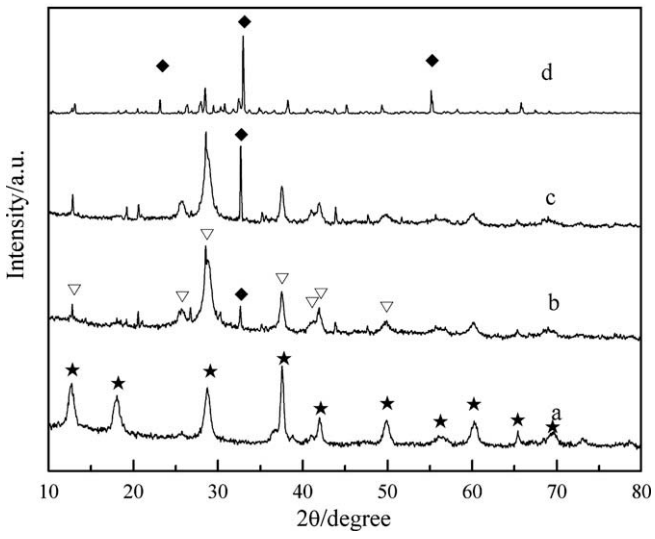

Fig. 2. XRD patterns of doped catalysts at different calcination temperature. (★) KMn_8O_{16}, JCPDS file 29-1020; (▽) $Pb_{2-x}Mn_8O_{16}$, JCPDS file 42-1349; (♦) bixbyite, JCPDS file 10-0069. (a) K-OMS-2, (b) Pb-OMS-2(B), (c) Pb-OMS-2(C) and (d) Pb-OMS-2(D).

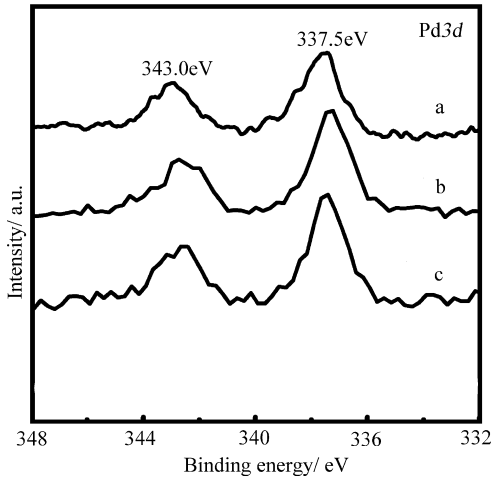

Fig. 3. XPS spectra of Pd3*d* (a) K-OMS-2, (b) Pb-OMS-2(A1) and (c) Pb-OMS-2(A2).

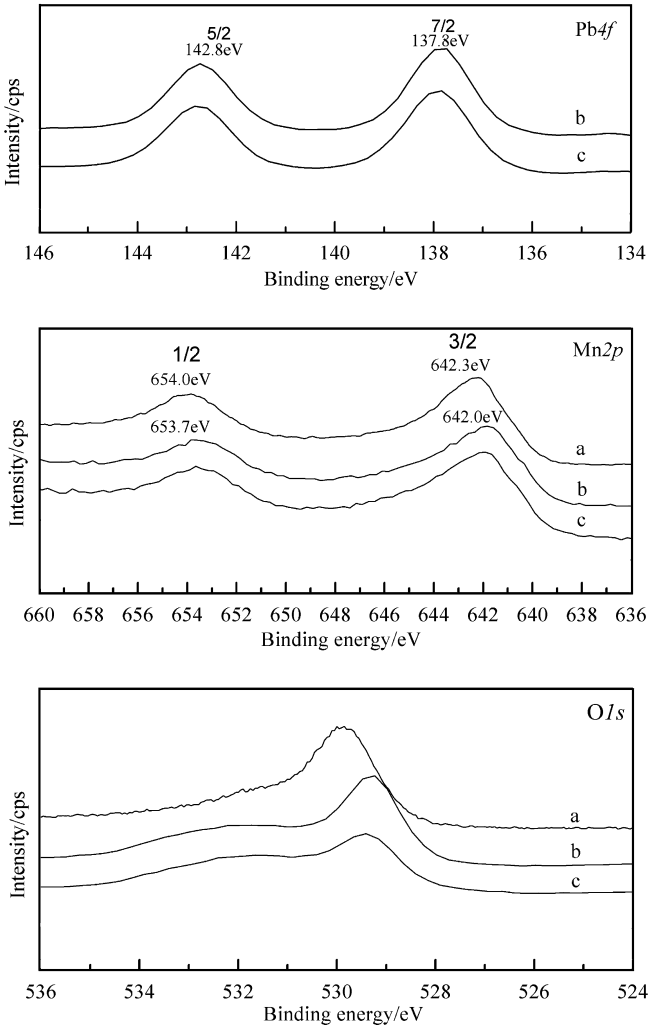

Fig. 4. XPS spectra of Pb4*f*, Mn2*p*, O1*s* (a) K-OMS-2, (b) Pb-OMS-2(A1) and (c) Pb-OMS-2(A2).

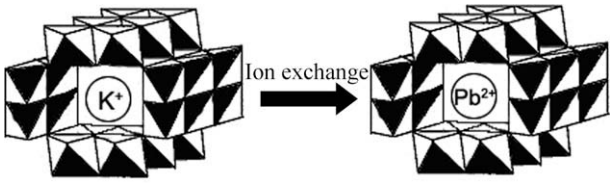

Fig. 5. Schematic diagram of transformation process of the crystal structure.

Table 2
Proportion of different oxygen species derived from fitted *O1s* spectrum.

Sample	O1s(eV)	FWHM[a]	%O
a	529.8	1.5	62.0 O^{2-}
K-OMS-2	531.6	2.3	33.3OH^-
	533.5	2.7	4.7 H_2O
b	529.2	1.3	49.2 O^{2-}
Pb-OMS-2(A1)	531.2	2.6	33.4 OH^-
	533.0	2.2	17.4 H_2O
c	529.3	1.5	46.7 O^{2-}
Pb-OMS-2(A2)	531.5	2.7	42.7 OH^-
	533.3	1.9	10.6 H_2O

[a] Full width at half maximum.

3.3. XPS characterization

XPS spectra showed further information on the structure of doped Pd/Pb-OMS-2 catalysts. Pd/K-OMS-2, Pd/Pb-OMS-2(A1) and Pd/Pb-OMS-2(A2) were selected as target samples considering interference of impure phase. Fig. 3 showed that no change in binding energy of Pd species was observed. The Pd*3d* binding energies at 337.5 eV and 343.0 eV were almost the same before and after the doping of Pb.

As summarized in Fig. 4, Pb$4f_{7/2}$ and Pb$4f_{5/2}$ of two doped catalysts were centered at 137.8 eV and 142.8 eV, respectively. They were attributed to Pb^{2+} in oxides and the possible Pb configuration in doped catalysts was Mn_2—O—Pb or Mn—O—Pb [14]. On the basis of Pb*4f* XPS spectrum and XRD analysis, we inferred that Pb^{2+} entered into the tunnels by replacing K^+ and no Pb^{2+} was oxidized to Pb^{4+} in the entire process. The transformation process of Pb-OMS-2 was schematically shown in Fig. 5.

XPS spectrum of Mn*2p* showed that the binding energies of Pb doped catalysts were about 0.3 eV lower than that of undoped catalysts. This small shift indicated the electronic densities of Mn atoms increased, which suggested the low-valence Mn species increased. Mn^{3+} was verified to be the low-valence Mn in K-OMS-2 and Pb-OMS-2 [15]. The lattice have been known to be strained when the tunnels K^+ was exchanged with smaller radius ions. Consequently, it was inferred that the substitution of K^+ (0.133 nm) with relatively smaller ionic radius Pb^{2+} (0.122 nm) also provoked the lattice strain and the increase of Mn^{3+} sites was one of the effects of the strain [16]. Considering that Mn^{3+} was more easily oxidized by oxygen than Mn^{2+}, the increase of Mn^{3+} benefited the replenishment of reduced Mn^{4+} in redox cycle and led to the enhanced activities of two Pb doped catalysts.

Mn^{3+} sites instead of Mn^{4+} could also originate a weak Mn-O bond, and this phenomenon may lead to the formation of active oxygen species in the lattice [17]. The corresponding spectra of oxygen species were presented in Fig. 4 O*1s* and the proportion of different oxygen species derived from fitted O*1s* spectrum was displayed in Table 2, which referring to the XPS results obtained by Peluso [17]. From Table 2, it can be seen that two Pd/Pb-OMS-2 samples possessed more molecular H_2O and OH^- compared with Pd/K-OMS-2. The literature reported that hollandite-type Pb-OMS-2 should contain more molecular H_2O because it had more unoccupied tunnel sites than cryptomelane-structure K-OMS-2 [15]. In view of charge equilibrium, OH^- species replaced O^{2-} with Mn^{3+} replacing Mn^{4+}. As a result, the increases of OH^- species was observed. On the one hand, H_2O was an inhibitor of the oxidative carbonylation of phenol; on the other hand, OH groups may be active oxygen species and hot oxygen-containing radicals like HOO^* generated according to Eq. $MnO_2 + H^+ + e^- \rightarrow MnOOH$, which was capable of oxidizing Pd^0[2]. Thus, a large proportion of OH groups and a small proportion of inhibitor H_2O were possible to interpret the highest activity of Pd/Pb-OMS-2(A2) catalyst among three samples.

4. Conclusion

The effects of Pb dopant on structure and activity of the palladium catalyst have been investigated for heterogeneous oxidative carbonylation of phenol to DPC without homogeneous cocatalyst. The DPC yield increased to 18.1% after the doping of Pb. This suggested that the new support of $Pb_{2-x}Mn_8O_{16}$ was responsible for the enhanced catalytic performance. Pb^{2+} replaced K^+ in tunnels through ion exchange, resulting in lattice strain and the changes of Mn valence and oxygen species. The increase of Mn^{3+} and the formation of more OH groups benefited the redox cycle between active Pd species and Pb doped supports.

Acknowledgements

We are grateful for the financial support from Natural Science Foundation of China (Grant No. 20906073) and Hubei Provincial Natural Science Foundation of China (Grant No. 2008CDA009).

References

[1] J.L. Gong, X.B. Ma, S.P. Wang, Appl. Catal. A 316 (2007) 1.
[2] J.L. Spivack, J.N. Cawse, D.W. Whisenhunt, B.F. Johnson, K.V. Sha-lyaev, J. Male, E.J. Pressman, J.Y. Ofori, G.L. Soloveichik, B.P. Patel, T.L. Chuck, D.J. Smith, T.M. Jordan, M.R. Brennan, R.J. Kilmer, E.D. Williams, Appl. Catal. A 254 (2003) 5.
[3] M. Goyal, R. Nagahata, J. Sugiyama, M. Asai, M. Ueda, K. Takeuchi, Catal. Lett. 54 (1998) 29.
[4] M. Takagi, H. Miyagi, T. Yoneyama, J. Mol. Catal. A: Chem. 129 (1998) 1.
[5] H.Y. Song, E.D. Park, J.S. Lee, J. Mol. Catal. A: Chem. 154 (2000) 243.
[6] G.Z. Fan, T. Li, X. Li, Appl. Organomet. Chem. 20 (2006) 656.
[7] K. Okuyama, J. Sugiyama, R. Nagahata, M. Asai, M. Ueda, K. Takeuchi, Green Chem. 5 (2003) 563.
[8] W. Xue, J.C. Zhang, Y.J. Wang, X.Q. Zhao, Q. Zhao, Catal. Commun. 6 (2005) 431.
[9] K.J.L. Linsen, J. Libens, P.A. Jacobs, Chem. Commun. (2002) 2728.
[10] Z.H. Li, Y.J. Wang, X.S. Ding, X.Q. Zhao, J. Nat. Gas Chem. 18 (2009) 104.
[11] M. Liu, Y.X. Wu, Z.P. Du, H. Yuan, J.W. Ge, Shiyou Huagong 37 (2008) 672.
[12] S. Sithambarama, L.P. Xu, C.H. Chen, Y.S. Ding, R. Kumara, C. Calverta, L.S. Steven, Catal. Today 140 (2009) 162.
[13] X. Chen, Y.F. Shen, S.L. Suib, C.L. O'Young, Chem. Mater. 14 (2002) 940.
[14] T. Boonfueng, L. Axe, Y. Xu, T.A. Tyson, J. Colloid Interf. Sci. 303 (2006) 87.
[15] J.E. Post, R.B. Von Dreele, P.R. Buseck, Acta Crystallogr. B 38 (1982) 1056.
[16] V.D. Makwana, L.J. Garces, J. Liu, J. Cai, Y.C. Son, L.S. Steven, Catal. Today 85 (2003) 225.
[17] M.A. Peluso, L.A. Gambaro, E. Pronsato, D. Gazzoli, H.J. Thomas, J.E. Sambeth, Catal. Today 133 (2008) 487.